^{99m}Tc-Labeled Divalent and Tetravalent CC49 Single-Chain Fv's: Novel Imaging Agents for Rapid In Vivo Localization of Human Colon Carcinoma

Apollina Goel, Janina Baranowska-Kortylewicz, Steven H. Hinrichs, James Wisecarver, Gabriela Pavlinkova, Sam Augustine, David Colcher, Barbara J.M. Booth, and Surinder K. Batra

Department of Biochemistry and Molecular Biology, Department of Radiation Oncology, and Department of Pathology and Microbiology, Eppley Institute for Research in Cancer and Allied Diseases, University of Nebraska Medical Center, Omaha, Nebraska; and Coulter Pharmaceutical Inc., San Francisco, California

Radioimmunopharmaceutical agents enabling rapid high-resolution imaging, high tumor-to-background ratios, and minimal immunogenicity are being sought for cancer diagnosis and imaging. Genetic engineering techniques have allowed the design of single-chain Fv's (scFv's) of monoclonal antibodies (mAbs) recognizing tumor-associated antigens. These scFv's show good tumor targeting and biodistribution properties in vivo, indicating their potential as imaging agents when labeled with a suitable radionuclide. **Methods:** Divalent (sc(Fv)$_2$) and tetravalent ([sc(Fv)$_2$]$_2$) scFv's of mAb CC49 were evaluated for radioimmunolocalization of LS-174T colon carcinoma xenografts in athymic mice. scFv's were radiolabeled with ^{99m}Tc by way of the bifunctional chelator succinimidyl-6-hydrazinonicotinate hydrochloride using tricine as the transchelator. The immunoreactivity and in vitro stability of the scFv's were analyzed after radiolabeling. Biodistribution and pharmacokinetic studies were performed to determine the tumor-targeting potential of the radiolabeled scFv's. Whole-mouse autoradiography illustrated the possible application of these ^{99m}Tc-labeled multivalent scFv's for imaging. **Results:** The radiolabeling procedure gave ≥95% radiometal incorporation, with a specific activity of >74 MBq/mg scFv. In solid-phase radioimmunoassay, both sc(Fv)$_2$ and [sc(Fv)$_2$]$_2$ exhibited 75%–85% immunoreactivity, with nonspecific binding between 0.8% and 1.2%. Size-exclusion high-performance liquid chromatography showed sc(Fv)$_2$ as a 60-kDa protein and [sc(Fv)$_2$]$_2$ as a 120-kDa protein. Blood clearance studies showed the elimination half-life of ^{99m}Tc-labeled sc(Fv)$_2$ as 144 min and that of [sc(Fv)$_2$]$_2$ as 307 min. Whole-body clearance studies confirmed the rapid elimination of scFv's, with half-lives of 184 ± 19 min for sc(Fv)$_2$ and 265 ± 39 min for [sc(Fv)$_2$]$_2$ ($P < 0.001$). At 6 h after administration, the tumor localization was 7.2 ± 0.7 percentage injected dose per gram of tumor (%ID/g) for ^{99m}Tc-sc(Fv)$_2$. ^{99m}Tc-[sc(Fv)$_2$]$_2$ showed a tumor uptake of 19.1 ± 1.1 %ID/g at the same time; the amount of radioactivity in the tumors was 4-fold higher than in the spleen and kidneys and 2-fold higher than in the liver. Macroautoradiography performed at 6 and 16 h after administration clearly detected the tumor with both scFv's. **Conclusion:** ^{99m}Tc-labeled multivalent scFv's show good tumor-targeting characteristics and high radiolocalization indices (tumor-to-background ratio). These reagents, therefore, have the potential for use in clinical imaging studies of cancer in the field of nuclear medicine.

Key Words: single-chain Fv; multivalency; ^{99m}Tc; biodistribution; macroautoradiography

J Nucl Med 2001; 42:1519–1527

Radioimmunoscintigraphy (RIS) combines the advantage of antibody specificity and the emission properties of the selected radionuclide for effective localization (*1*). Imaging with radiolabeled IgGs typically occurs at 3–10 d after administration, because IgGs, being large glycoproteins (approximately 150 kDa), persist in the blood for an extended time, resulting in a high systemic background radioactivity in patients (*2*). IgGs also show poor diffusion from the vasculature into the tumor (*3*). Furthermore, administration of whole xenogenic antibody to patients can elicit an immune reaction known as the human antimouse antibody response, precluding multiple RIS studies in individual patients (*4*).

The 2 main characteristics dictating the targeting potential of an antibody-based reagent are the size relative to the renal threshold for first-pass elimination and the functional avidity of the molecule. Antibody fragments F(ab′)$_2$, when radiolabeled with ^{99m}Tc or ^{123}I, produce better images because of their more rapid clearance from nontarget tissues and also appear to be less immunogenic to the host recipient (*5*). However, production of stable and clinical-grade purified antibody fragments such as F(ab′)$_2$ and Fab′ remains tedious. ^{99m}Tc-labeled Fab′ fragments such as IMMU-4

Received Oct. 26, 2000; revision accepted Feb. 20, 2001.

For correspondence or reprints contact: Surinder K. Batra, PhD, Department of Biochemistry and Molecular Biology, Eppley Institute for Research in Cancer and Allied Diseases, University of Nebraska Medical Center, 984525 Nebraska Medical Center, Omaha, NE 68198-4525.

Fab′ (CEA-Scan; Immunomedics, Inc., Morris Plains, NJ) (*6*) and LL2 Fab′ (*7*) have improved the RIS results in patients, with imaging typically occurring 4–5 h after injection. The radiolabeled Fab′, being monovalent, shows lower absolute tumor uptake than does whole IgG and can result in kidney radiotoxicity (*5*,*8*,*9*).

Genetic engineering methods have been used to construct single-chain Fv's (scFv's) containing the variable regions of the light chain (V_L) and heavy chain (V_H) connected by a flexible linker (*10*,*11*). This antibody moiety (approximately 30 kDa) retains full antigen-binding capacity, clears rapidly from the whole body and from blood (*11*,*12*), and better penetrates the tumor (*13*). ScFv's have had high radiolocalization indices (tumor–to–normal-tissue ratio) with minimal retention in the normal tissue (*9*), making them suitable for diagnostic applications (*14*). Moreover, when compared with intact mAb's, scFv's may be less immunogenic because they lack the Fc portion of murine antibodies, the site of antigenic determinants for human antimouse antibody (*15*). ScFv's therefore hold the advantage of allowing multiple imaging.

We have engineered scFv's of the mAb CC49, which selectively recognizes a unique sialyl-Tn epitope of tumor-associated glycoprotein–72 expressed on a variety of human adenocarcinomas (*16*). The divalent sc$(Fv)_2$ was constructed by joining V_L and V_H, in tandem, using the 205C linker (*17*). Sc$(Fv)_2$ spontaneously dimerized to form tetravalent $[sc(Fv)_2]_2$ (*18*). Multivalent scFv's, when radiolabeled with ^{125}I or ^{131}I, showed improved biodistribution and pharmacokinetics over monovalent CC49 scFv and over the prototype IgG antibody and its enzymatic fragments (*9*,*17*,*18*).

In this study, the biodistribution and radioimmunolocalization characteristics of ^{99m}Tc-sc$(Fv)_2$ and ^{9m}Tc-$[sc(Fv)_2]_2$ were analyzed in athymic mice bearing LS-174T human colon carcinoma xenografts. The results indicate that multivalent scFv's, when radiolabeled with ^{99m}Tc, can enable the rapid acquisition of tumor images because of optimum biologic half-life and functional affinity.

MATERIALS AND METHODS

Purification and Characterization of Multivalent CC49 scFv's in *Pichia pastoris*

The divalent scFv construct sc$(Fv)_2$ (V_L-linker-V_H-linker-V_L-linker-V_H-His_6) was derived from murine mAb CC49, cloned in the yeast expression vector pPICZαA (Invitrogen, Carlsbad, CA), and transformed into competent *P. pastoris* KM71 cells (*his4arg4aox1*Δ*::ARG4*) (*17*). On expression, sc$(Fv)_2$ associated spontaneously to form noncovalent tetrameric $[sc(Fv)_2]_2$ (*18*). The scFv's were purified by immobilized metal affinity chromatography using the chelating resin Ni^{++}-nitrilotriacetic acid Superflow (Qiagen Inc., Valencia, CA). sc$(Fv)_2$ and $[sc(Fv)_2]_2$ were separated using a Superdex 200 column (1.6 × 60 cm; Pharmacia, Piscataway, NJ) (*17*,*18*). The protein concentration was determined by the method of Lowry et al. (*19*).

Sodium dodecylsulfate–polyacrylamide gel electrophoresis (SDS-PAGE) of scFv's was performed according to the method of Laemmli (*20*) under reducing and nonreducing conditions. The gels were stained with Coomassie blue R-250 (Bio-Rad Laboratories Inc., Hercules, CA). High-performance liquid chromatography (HPLC) analysis was performed on TSK G2000SW and TSK G3000SW (Toso Haas, Tokyo, Japan) columns connected in series with 67 mmol/L sodium phosphate buffer, pH 6.8, with 100 mmol/L KCl as the mobile phase. The columns were calibrated with a gel filtration calibration kit (Bio-Rad) using thyroglobulin (670 kDa), γ-globulin (158 kDa), ovalbumin (44 kDa), myoglobin (17 kDa), and vitamin B-12 (1.35 kDa). The elution was monitored by an in-line ultraviolet detector at 280 nm.

Determination of Immunoreactivity and Affinity Constants of scFv's

The immunoreactivity of unlabeled scFv's was analyzed by a solid-phase competition enzyme-linked immunosorbent assay (ELISA), using either bovine submaxillary gland mucin (BSM; Sigma, St. Louis, MO) as the representative for tumor-associated glycoprotein–72 antigen or bovine serum albumin (BSA) as the negative control (*9*). Briefly, a 5-μL portion of the test samples, in 3-fold serial dilutions, was incubated with 6 ng per well of biotinylated CC49 IgG. The binding was detected with alkaline phosphate–conjugated streptavidin (Jackson ImmunoResearch Laboratories, Inc., West Grove, PA) and *p*-nitrophenyl phosphate substrate. The binding affinities of sc$(Fv)_2$ and $[sc(Fv)_2]_2$ to BSM were determined by surface plasmon resonance measurements using an upgraded version of BIAcore 1000 (Pharmacia Biosensor, Uppsala, Sweden) as described previously (*17*,*18*).

Radiolabeling

Tricine and stannous chloride dihydrate were obtained from Aldrich (Milwaukee, WI). The hydrazinonicotinamide chelator was prepared as *N*-hydroxysuccinimide ester of the chelator (succinimidyl-6-hydrazinonicotinate hydrochloride [SHNH]) (*21*). The ^{99m}Tc-pertechnetate was obtained from a ^{99}Mo–^{99m}Tc radionuclide generator (Syncor Corp., Omaha, NE). The radiolabeling was accomplished using the standard operating protocol. Briefly, the hydrazino-modification of scFv's was achieved by reacting scFv with SHNH at a molar ratio of 10:1 in 100 mmol/L sodium phosphate buffer, pH 7.8, in the dark at 4°C overnight. The unreacted SHNH was removed using a Sephadex G-10 column (Pharmacia) with an elution consisting of 100 mmol/L saline, pH 5.2, buffered with 20 mmol/L sodium citrate. The substitution ratio was calculated as follows: number of SHNH groups/molecule of scFv = percentage of protein-bound ^{99m}Tc × 10/100. For radiolabeling, 37 MBq ^{99m}Tc-labeled sodium pertechnetate, 100 μg tricine (at a concentration of 20 mg/mL), and 25 μg stannous chloride (prepared fresh at 5 mg/mL in water) were added and allowed to react for 15 min at room temperature. Four hundred micrograms of SHNH-derivatized scFv's were added, and the reaction was incubated at room temperature for 45 min. The radiolabeled scFv's were separated from free pertechnetate using a Sephadex G-25 column (Pharmacia). The percentage of ^{99m}Tc bound to the protein was determined by instant thin-layer chromatography using 150 mmol/L sodium acetate, pH 5.8, or 1:4 methanol:water (v/v) as the solvent.

Characterization of Radiolabeled scFv's

Radiolabeled proteins were analyzed by SDS-PAGE, and the radioactivity associated with the protein bands was measured using the ImageQuant software of a PhosphorImager system (Molecular Dynamics, Sunnyvale, CA). For determining the integrity of scFv's after radiolabeling, analytic size-exclusion HPLC was per-

formed. Fractions (1 mL) of the radiolabeled protein were collected, and the radioactivity was determined in a Minaxi Auto-Gamma 5000 γ-counter (Packard Instrument Co., Meriden, CT). Radioimmunoassay was used for assessing the immunoreactivity of the radiolabeled CC49 scFv forms in which BSM or BSA was attached to a solid-phase matrix (Reacti-Gel HW-65F; Pierce Chemical Co., Rockford, IL) (*9*).

In Vitro Stability Studies

For assessing the in vitro stability of the radiolabeled scFv's, ^{99m}Tc-sc(Fv)$_2$ or ^{99m}Tc-[sc(Fv)$_2$]$_2$ was incubated at a concentration of 0.05 mg/mL at 37°C in 1% BSA or 1% mouse serum for 24 h. Samples were removed periodically for HPLC analysis, and the percentage of radioactivity associated with the protein peaks was calculated.

Biodistribution Studies

For in vivo studies, the human colon carcinoma LS-174T cell line (4×10^6 cells; American Type Culture Collection, Manassas, VA) was implanted subcutaneously in female athymic mice (nu/nu, 4–6 wk old; Charles River Laboratories, Wilmington, MA). The mice were used after 6–8 d, when the tumor volume reached approximately 250–300 mm^3. Biodistribution studies were performed after injection of 0.37 MBq ^{99m}Tc-sc(Fv)$_2$ or ^{99m}Tc-[sc(Fv)$_2$]$_2$ through the tail vein. At specified times after administration, mice (3 per group) were euthanized and major organs were excised, weighed, and counted in the Minaxi γ-counter. The percentage of the injected dose per gram of tissue (%ID/g) was calculated, and the radiolocalization indices (ratio of %ID/g in tumor to %ID/g in normal tissue) were determined.

For the whole-body retention studies, mice bearing the LS-174T xenografts (3 mice per group) received an injection of 0.37 MBq ^{99m}Tc-labeled scFv's through the tail vein. The whole-body radioactivity was determined at various times after injection in a custom-built NaI crystal (*9,17,18*). The data were fitted into a monoexponential equation with a bolus injection as an experimental model. The clearance rates were compared for differences between means using a 2-tailed Student *t* test. The blood clearance property of radiolabeled scFv's was studied by injecting 0.74 MBq ^{99m}Tc-sc(Fv)$_2$ or ^{99m}Tc-[sc(Fv)$_2$]$_2$ into tumor-bearing mice. Blood samples (5 μL) were obtained through the tail vein at various times after administration and were counted for radioactivity. The data were fitted into a biexponential equation, and the half-lives were calculated using a numeric module of the SAAM II computer program (SAAM Institute, Inc., Seattle, WA) for kinetic analysis.

Macroautoradiography

For radioimmunolocalization studies, tumor-bearing mice received a 3.7-MBq intravenous injection of ^{99m}Tc-labeled sc(Fv)$_2$ or [sc(Fv)$_2$]$_2$. At 6 and 16 h after administration, the mice (3 per group) were euthanized. The major visceral organs were excised en bloc along with the tumor, and the animal was reconstructed. The organ block was frozen by immersion in a bath of dry ice and acetone (−70°C). Whole-body cryosections (50 μm) were cut at −20°C sagittally using a cryomicrotome (Microm, Heidelberg, Germany). The cryosections were transferred to Superfrost Plus slides (Fisherbrand, Pittsburgh, PA), and the radioactivity was detected using ImageQuant. The radioactivity was quantified by averaging 3 selected areas of equal volume per organ or tumor and calculating the pixels (densitometric scores) above the background using ImageQuant. Alternate sections (10 μm) were stained with hematoxylin–eosin and viewed under the light microscope.

RESULTS

In Vitro Characterization of Multivalent CC49 scFv's

Figure 1 is a schematic representation of various scFv's that we have developed. The divalent sc(Fv)$_2$ was constructed using the 205C linker in a *P. pastoris* expression system and purified from the secreted medium using immobilized metal affinity chromatography (*17*). On expression, 20%–30% of sc(Fv)$_2$ (approximately 60 kDa) formed tetramers ([sc(Fv)$_2$]$_2$; approximately 120 kDa) or higher aggregates (>200 kDa) by noncovalent interactions (*18*). SDS-PAGE of scFv's showed the preparations to be >95% pure. Both sc(Fv)$_2$ and [sc(Fv)$_2$]$_2$ migrated as a single band of approximately 60 kDa under reducing and nonreducing conditions. Size-exclusion HPLC showed that the molecular weights of sc(Fv)$_2$ and [sc(Fv)$_2$]$_2$ were 60 kDa and 120 kDa, respectively. Competitive ELISA confirmed the immunoreactivity of both the proteins. The binding parameters derived from a real-time kinetic study using a BIAcore instrument were association rate (k_{on}) = 2.2×10^4 $M^{-1}s^{-1}$, dissociation rate (k_{off}) = $8.0 \times 10^{-4}s^{-1}$, and association constant (K_A) = 2.8×10^7 M^{-1} for sc(Fv)$_2$, as reported earlier (*17*). [sc(Fv)$_2$]$_2$ showed $k_{on} = 9.1 \times 10^4$ $M^{-1}s^{-1}$, $k_{off} = 8.9 \times 10^{-4}s^{-1}$, and $K_A = 1.0 \times 10^8$ M^{-1} (*18*).

The hydrazino-modified scFv's used in the studies showed approximately 2.3 SHNH groups per sc(Fv)$_2$ and approximately 2.8 SHNH groups per [sc(Fv)$_2$]$_2$. Both sc(Fv)$_2$ and [sc(Fv)$_2$]$_2$, when radiolabeled with ^{99m}Tc, showed a specific activity of 74–111 MBq/mg scFv, with >95% of ^{99m}Tc bound to the scFv's. After radiolabeling, the scFv's were evaluated for any changes in stability and immunoreactivity. On SDS-PAGE under nonreducing and reducing conditions, approximately >90% of the total radioactivity was found to be associated with the protein band of 58 kDa for both sc(Fv)$_2$ (Fig. 2, lanes 1 and 3) and [sc(Fv)$_2$]$_2$ (Fig. 2, lanes 2 and 4). HPLC analysis also showed ≥95% of the radiometal as ^{99m}Tc-sc(Fv)$_2$ (60 kDa) and ^{99m}Tc-[sc(Fv)$_2$]$_2$ (120 kDa) (Fig. 3). The immunoreactivity of ^{99m}Tc-labeled scFv's by solid-phase radioimmunoassay was 85%–95%, with a nonspecific binding between 0.8% and 1.5%.

Stability of ^{99m}Tc-Labeled CC49 scFv's

By HPLC studies, a <20% loss of radiolabel for both ^{99m}Tc-sc(Fv)$_2$ and ^{99m}Tc-[sc(Fv)$_2$]$_2$ was detected at 24 h in vitro when incubated at 37°C with 1% BSA (Table 1). However, on incubation of the radiolabeled multivalent scFv's for 24 h in the presence of 1% mouse serum, approximately 20% and 10% of the ^{99m}Tc were found associated with low-molecular-weight (<50 kDa) proteins and high-molecular-weight (>130 kDa) proteins, respectively. The observation suggested the possibility of aggregation of the radiolabel with serum proteins (Table 1). For [sc(Fv)$_2$]$_2$, approximately 10% radioactivity was found as 60 kDa at 24 h in mouse serum, probably because of the dissociation of tetramers to dimers.

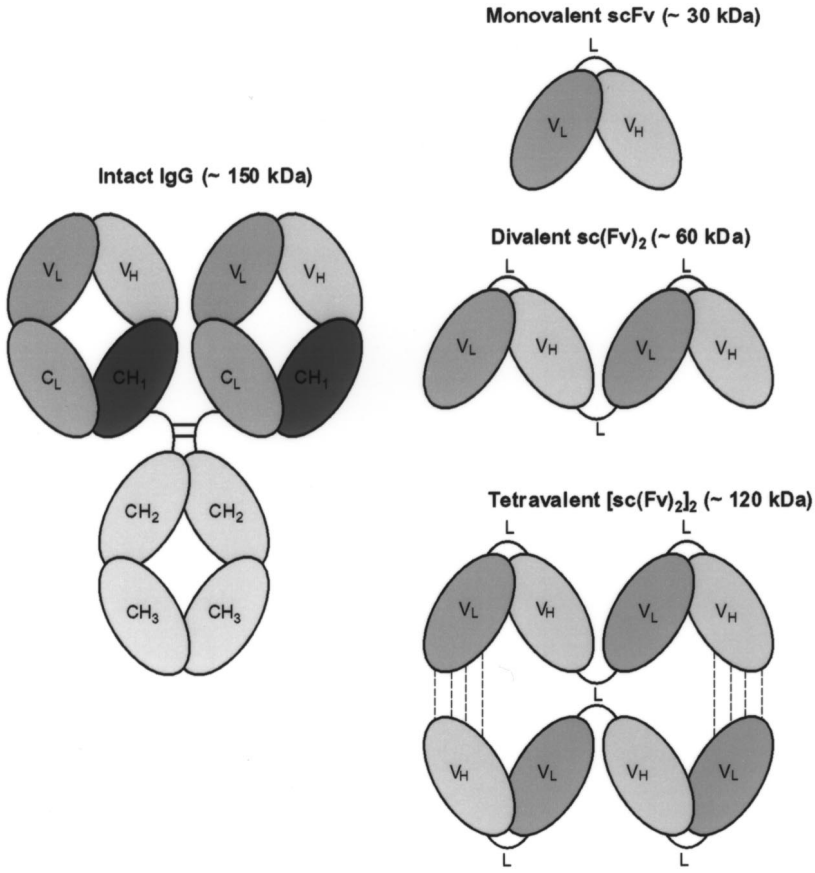

FIGURE 1. Schematic representation of IgG and various scFv's developed for improved radioimmunodetection of colon carcinoma. Monovalent scFv consists of V_L and V_H domains of mAb CC49 joined by 205C linker (*40*). Two monovalent scFv's were connected in tandem, at nucleotide level, to obtain divalent sc(Fv)$_2$ (*17*). Tetravalent [sc(Fv)$_2$]$_2$ was formed by noncovalent association of sc(Fv)$_2$ (*18*). C_L = constant region domain for light chain; L = linker.

Pharmacokinetics and Biodistribution Studies

The in vivo tumor-targeting properties of ^{99m}Tc-labeled scFv's were evaluated through pharmacokinetic and biodistribution studies on athymic mice bearing LS-174T colon carcinoma xenografts. As shown in Figure 4, the elimination half-lives for ^{99m}Tc-sc(Fv)$_2$ and ^{99m}Tc-[sc(Fv)$_2$]$_2$ were 144 min and 307 min, respectively. Similar trends were observed for the whole-body clearance studies, with half-lives of 184 ± 19 min for sc(Fv)$_2$ and 265 ± 39 min for [sc(Fv)$_2$]$_2$ ($P < 0.001$). Biodistribution studies are summarized in Table 2. ^{99m}Tc-conjugated scFv's exhibited good tumor targeting: sc(Fv)$_2$ showed 7.2 ± 0.7 %ID/g and 2.3 ± 0.1 %ID/g at 6 h and 16 h, respectively, after administration, whereas [sc(Fv)$_2$]$_2$ exhibited 19.1 ± 1.1 %ID/g and 7.6 ± 0.2 %ID/g at the respective time points (Table 2). The blood level of ^{99m}Tc-[sc(Fv)$_2$]$_2$ was approximately 2-fold higher than that of ^{99m}Tc-sc(Fv)$_2$ at all time points (Table 2). An elevated uptake, besides being detected in tumors, was detected in the kidneys, liver, and spleen with both of the radiolabeled scFv's (Table 2). At 6 h after administration, the kidneys showed a 3-fold higher retention of sc(Fv)$_2$ (18.8 ± 0.1 %ID/g) than of [sc(Fv)$_2$]$_2$ (5.6 ± 0.2 %ID/g) (Table 2). The uptake of radiometal in the liver and spleen was found to be similar for sc(Fv)$_2$ and [sc(Fv)$_2$]$_2$ at 6 h after administration, with values of 10.4 ± 0.7 %ID/g and 11.7 ± 0.7 %ID/g, respectively, for the liver and 8.0 ± 0.9 %ID/g and 5.5 ± 0.2 %ID/g, respectively, for the spleen (Table 2).

To assess the diagnostic potential of ^{99m}Tc-labeled scFv's, we determined the radiolocalization index (%ID/g of tumor divided by %ID/g of normal tissue). At 16 h after administration, the radiolocalization indices for well-perfused organs such as the liver and the spleen were 1.4 and 1.5, respectively, for sc(Fv)$_2$ and 2.5 and 5.6, respectively, for [sc(Fv)$_2$]$_2$ (Table 3). At 16 h after administration, the tumor-to-blood ratios were 4.6:1 for ^{99m}Tc-sc(Fv)$_2$ and 12.7:1 for ^{99m}Tc-[sc(Fv)$_2$]$_2$. The tissue-to-blood ratios for liver, kidneys, and spleen were 3:1, 7:1, and 3:1, respectively, for ^{99m}Tc-sc(Fv)$_2$ and 4:1, 3:1, and 2:1, respectively, for ^{99m}Tc-[sc(Fv)$_2$]$_2$. ^{99m}Tc-[sc(Fv)$_2$]$_2$ therefore showed approximately 3-fold higher tumor localization than did ^{99m}Tc-sc(Fv)$_2$ at 16 h after administration.

Macroautoradiography

To determine the possibility of using the radiolabeled scFv's for immunolocalization studies, we obtained autoradiographic images from sagittal sections of the tumor-bearing mice that were euthanized 6 or 16 h after administration of ^{99m}Tc-sc(Fv)$_2$ (Figs. 5A and 5B) or ^{99m}Tc-[sc(Fv)$_2$]$_2$ (Figs. 5C and 5D). The autoradiographs confirmed a high degree of tumor localization and negligible retention in the blood and normal organs, the exceptions being the liver and pancreas. On quantitation (pixels above background) of radioactivity in sagittal sections of tumor-bearing athymic mice that received ^{99m}Tc-sc(Fv)$_2$, approximately a 2-fold

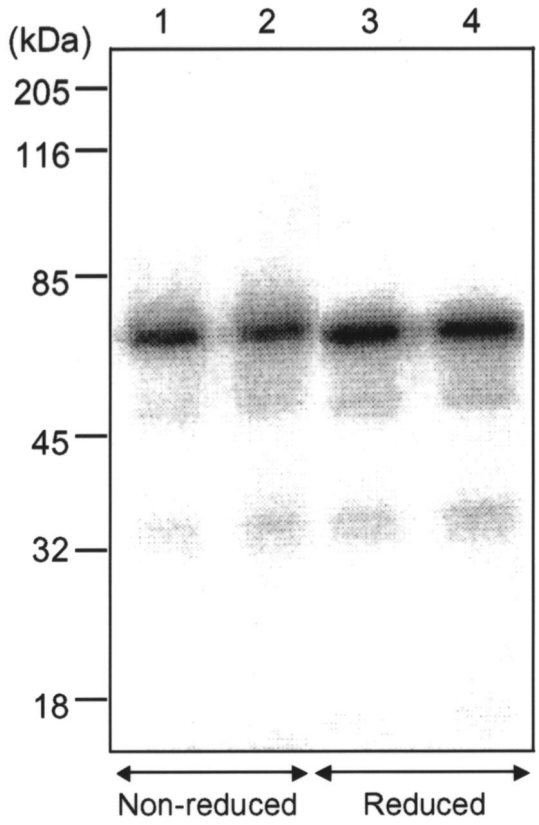

FIGURE 2. SDS-PAGE analysis of ^{99m}Tc-labeled divalent and tetravalent CC49 scFv's under nonreducing and reducing conditions. Sc(Fv)$_2$ = lanes 1 and 3; [sc(Fv)$_2$]$_2$ = lanes 2 and 4.

TABLE 1
The In Vitro Stability of ^{99m}Tc-Labeled Divalent and Tetravalent CC49 scFv's

% radioactivity in . . .	In vitro incubation at 37°C for 24 h			
	sc(Fv)$_2$		[sc(Fv)$_2$]$_2$	
	1% BSA	1% mouse serum	1% BSA	1% mouse serum
>130 kDa	2.5	8.9	3.2	6.4
[sc(Fv)$_2$]$_2$	—	—	81.6	65.2
sc(Fv)$_2$	85.6	74.5	2.5	10.2
<50 kDa	11.9	16.6	12.7	18.2

Radiolabeled scFv's (0.05 mg/mL) were incubated in either 1% BSA or 1% mouse serum and analyzed on HPLC column. Percentage of radioactivity associated with various peaks was calculated.

increase in tumor was observed over liver and pancreas at both 6 h and 16 h after administration. For ^{99m}Tc-[sc(Fv)$_2$]$_2$, approximately 2- and 5-fold increases were observed in the radioactivity measured per pixel at 6 h and 16 h, respectively. The tumor remained positive at 16 h after injection, with decreased background activity for both scFv's (Figs. 5B and 5D). The autoradiographic images were consistent with the tissue distribution data shown in Table 2.

DISCUSSION

scFv's are entering clinical trials for cancer diagnosis because they offer the advantage of high diffusion capacity;

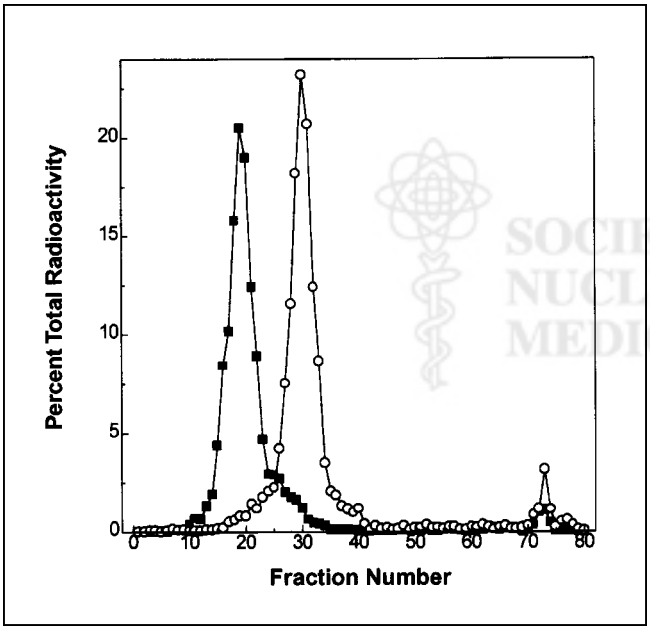

FIGURE 3. HPLC size-exclusion profiles of ^{99m}Tc-labeled divalent and tetravalent CC49 scFv's. Samples were analyzed using tandem of TSK G2000SW and TSK G3000W size-exclusion columns. Radiolabeled sc(Fv)$_2$ (○) and [sc(Fv)$_2$]$_2$ (■) eluted as single peaks, with >95% radioactivity associated with protein peaks.

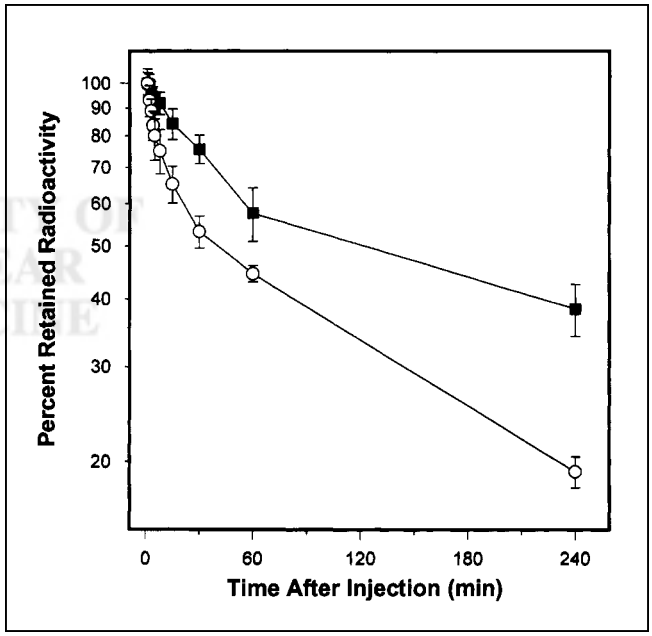

FIGURE 4. Pharmacokinetics of blood-pool clearance of ^{99m}Tc-sc(Fv)$_2$ (○) and ^{99m}Tc-[sc(Fv)$_2$]$_2$ (■) in athymic mice bearing LS-174T colon carcinoma xenografts. Average of 3 mice per group is presented. Values are not corrected for decay of radionuclide.

TABLE 2
Biodistribution of Divalent and Tetravalent scFv's of mAb CC49 (%ID/g) in Athymic Mice Bearing LS-174T Colon Carcinoma Xenografts

Tissue	Time (h)					
	0.5	1	4	6	16	24
$sc(Fv)_2$						
Tumor	9.9 ± 0.7	10.9 ± 0.8	12.6 ± 0.4	7.2 ± 0.7	2.3 ± 0.1	1.2 ± 0.0
Blood	13.9 ± 1.1	9.0 ± 0.2	4.3 ± 0.2	1.2 ± 0.1	0.5 ± 0.0	0.1 ± 0.0
Liver	18.9 ± 1.5	15.0 ± 1.1	14.8 ± 1.3	10.4 ± 0.7	1.7 ± 0.1	1.2 ± 0.0
Spleen	13.4 ± 1.2	11.3 ± 1.0	9.7 ± 0.7	8.0 ± 0.9	1.5 ± 0.0	1.0 ± 0.0
Kidneys	33.9 ± 1.8	30.1 ± 0.4	27.3 ± 1.4	18.8 ± 0.1	3.5 ± 0.1	2.4 ± 0.3
Lungs	5.4 ± 0.8	3.9 ± 0.6	1.3 ± 0.0	0.9 ± 0.0	0.1 ± 0.0	0.0 ± 0.0
$[sc(Fv)_2]_2$						
Tumor	13.3 ± 1.4	14.5 ± 0.9	15.0 ± 1.2	19.1 ± 1.1	5.6 ± 0.2	2.5 ± 0.0
Blood	27.3 ± 1.5	18.0 ± 1.0	7.5 ± 0.5	2.9 ± 0.1	0.6 ± 0.0	0.1 ± 0.0
Liver	18.0 ± 1.3	19.2 ± 1.2	20.1 ± 1.1	11.7 ± 0.7	2.2 ± 0.1	1.6 ± 0.0
Spleen	13.2 ± 0.8	14.6 ± 0.3	10.9 ± 0.5	5.5 ± 0.2	1.0 ± 0.1	1.0 ± 0.1
Kidneys	17.2 ± 0.5	16.5 ± 0.3	14.3 ± 1.9	5.6 ± 0.2	2.0 ± 0.0	1.1 ± 0.0
Lungs	7.2 ± 1.1	3.5 ± 0.6	2.7 ± 0.5	1.3 ± 0.1	0.2 ± 0.0	0.1 ± 0.0

^{99m}Tc-labeled $sc(Fv)_2$ or $[sc(Fv)_2]_2$ was injected into athymic mice (3 per group) bearing LS-174T tumors. Mice were killed at indicated times, and %ID/g of tumor, blood, and selected normal tissues was determined. %ID/g values presented are not corrected for decay of radioisotope. SEM for samples was determined. Experiment was repeated twice, and similar results were obtained.

fast elimination from the blood pool, leading to high-contrast imaging; and reduced immunogenicity (*22*,*23*). In a clinical study by Larson et al. (*24*), ^{123}I-labeled CC49 scFv detected primary and metastatic liver lesions of colorectal carcinoma; however, the images were suboptimal because of the low uptake of scFv by tumors. With phage technology, high-affinity scFv's have been generated to improve the tumor localization of scFv's (*25*,*26*). Divalent scFv's have been evaluated for improved tumor localization because of increased avidity and longer biologic half-life. Using ^{123}I-labeled anticarcinoembryonic antigen diabodies, Wu et al. (*27*) imaged 0.12- to 0.48-g tumors at 6 h after administration and showed, on the basis of the imaging figure of merit, that diabodies are a better choice for radioimaging than are monomers. Micro-PET imaging of LS-174T human colon carcinoma xenografts with ^{64}Cu-labeled 80-kDa dimers (minibody, scFv-C_H3) has been performed at 5 h after injection, with improved image qualities at 12–24 h after injection (*28*).

TABLE 3
Comparative Biodistribution Studies of ^{99m}Tc-Labeled Divalent and Tetravalent CC49 scFv's 16 Hours After Administration

Tissue	Radiolocalization index			
	$sc(Fv)_2$		$[sc(Fv)_2]_2$	
	6 h	16 h	6 h	16 h
Blood	6.0	4.6	6.6	9.3
Liver	0.7	1.4	1.6	2.5
Spleen	0.9	1.5	3.5	5.6
Kidneys	0.4	0.7	3.4	2.8
Lungs	8.0	23.0	14.7	28.0

^{99m}Tc-$sc(Fv)_2$ or ^{99m}Tc-$[sc(Fv)_2]_2$ was injected in athymic mice (3 per group) bearing LS-174T colon carcinoma xenografts. Mice were killed at fixed times, and radiolocalization indices (%ID/g of tumor divided by %ID/g of normal tissue) were determined.

To our knowledge, ours is the first study in which divalent and tetravalent scFv's have been evaluated for radioimmunodetection of human colon carcinoma xenografts after radiolabeling with ^{99m}Tc. For imaging using antibody fragments such as Fab′ and scFv, ^{99m}Tc (half-life, 6 h; 140 keV, 90%) appears to be the radioisotope of choice because its physical half-life is comparable with the biologic half-life of these carrier proteins. Radiolabeling of scFv with ^{99m}Tc involves chemical modification, genetic incorporation of Gly_4Cys peptide or His-tag as the ^{99m}Tc-chelation site, or insertion of a C-terminal cysteine. In this study, a bifunctional chelating agent (i.e., the SHNH ligand) was used in which the 6-hydrazinonicotinate forms the radiometal binding part and *N*-hydroxysuccinimide active ester forms amide linkages with the ϵ-amino groups of lysine residues. A comparison of antibody radiolabeling with ^{99m}Tc using the direct method and chelators such as *S*-benzoylmercaptoacetyltriglycine, TechneScan-HIG (Mallinckrodt Medical, Hennef, Germany), or SHNH showed that IgGs radiolabeled with ^{99m}Tc using SHNH exhibit improved serum stability and tumor-targeting properties (*29*,*30*). Antibodies radiolabeled with ^{99m}Tc using SHNH have been used for clinical imaging studies (*31*,*32*).

An indirect-labeling technique was used in which conjugation of SHNH to the scFv's occurred first and was followed by labeling with ^{99m}Tc through ligand exchange using the ^{99m}Tc

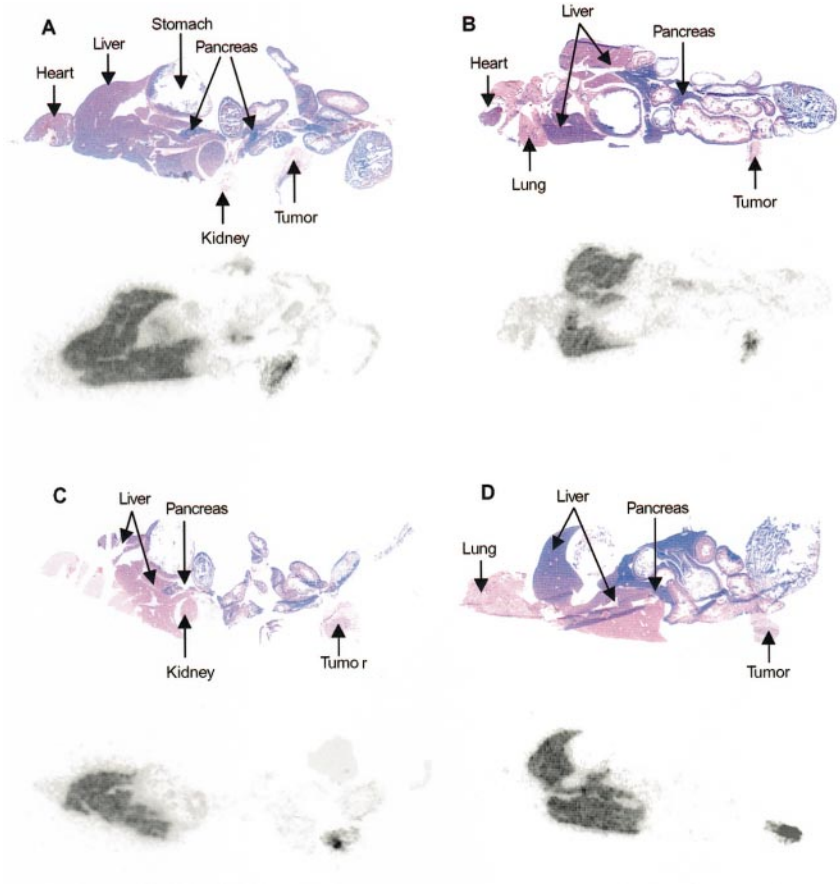

FIGURE 5. Sagittal section autoradiography of athymic mice bearing LS-174T human colon carcinoma xenografts injected with either ^{99m}Tc-sc(Fv)$_2$ or ^{99m}Tc-[sc(Fv)$_2$]$_2$. Autoradiography was performed at 6 and 16 h after administration of 3.7 MBq sc(Fv)$_2$ (A and B) or [sc(Fv)$_2$]$_2$ (C and D). Corresponding sections stained with hematoxylin–eosin show locations of major organs.

precursor complex ^{99m}Tc-tricine. Recently, for ^{99m}Tc radiolabeling of His-tagged scFv's, a novel method involving the use of organometallic aquaion $[^{99m}Tc(H_2O)_3(CO)_3]^+$ was reported (*33*). Because the multivalent CC49 scFv's used in this study contained a C-terminal His-tag, this radiolabeling technique was also tested. However, the labeling efficiency was poor (approximately 30%), probably because the procedure requires interaction between technetium carbonyl and ligand solution at a high temperature (75°C for 30 min).

In RIS, the use of stable radioimmunoconjugates to improve the radiolocalization index and acquire good images is extremely important. In this study, the ^{99m}Tc-labeled scFv's were found to be stable in vitro at 37°C for 24 h with 1% BSA. However, a radiolabel loss of approximately 30% at 24 h was observed when ^{99m}Tc-labeled scFv's were incubated with 1% mouse serum. ^{99m}Tc-labeled antibody fragments undergo transchelation in vivo with endogenous sulfhydryl compounds such as cysteines (Cys–^{99m}Tc–Cys) (*34*) and glutathione (^{99m}Tc-glutathione) (*35*). Behr et al. (*5*) suggested that ^{99m}Tc is less stable in fragments than in complete IgGs, possibly for stearic reasons. At 24 h with 1% mouse serum, approximately 9% of ^{99m}Tc was found to be associated with >130-kDa proteins. The presence of high-molecular-weight species has been reported with SHNH-labeled antibodies (*35*). Time-course HPLC analysis of serum samples of mice receiving ^{99m}Tc-labeled sc(Fv)$_2$ or [sc(Fv)$_2$]$_2$ showed that the radioisotope remained associated with the 60-kDa and 120-kDa proteins, respectively, until 2 h, indicating that no transchelation to other serum proteins occurred in vivo at earlier times.

In biodistribution studies at 6 h after administration, ^{99m}Tc-labeled sc(Fv)$_2$ and [sc(Fv)$_2$]$_2$ showed tumor localizations of 7.2 ± 0.7 %ID/g and 19.1 ± 1.1 %ID/g, respectively. Accretion of radiometal in normal organs such as the kidneys and liver was found to be significantly high (Table 2). Nevertheless, the ^{99m}Tc-labeled [sc(Fv)$_2$]$_2$ exhibited a specific localization to LS-174T tumors ≥6 h after administration, as observed earlier for the radioiodine-labeled multivalent scFv's (*17,18*). Under in vivo conditions, ^{99m}Tc can be transferred to cysteine and cleared by the kidneys (*36*). Alternatively, ^{99m}Tc can bind to glutathione in the liver and be released into the hepatobiliary tree and eliminated through the kidneys as a cysteine adduct (*36*). Therefore, the pronounced nonspecific localization of ^{99m}Tc in the liver and kidneys observed in this study was not surprising. In the kidneys, accumulation of ^{99m}Tc-[sc(Fv)$_2$]$_2$ was about 3-fold less than accumulation of ^{99m}Tc-sc(Fv)$_2$ because molecules that are ≤60 kDa undergo glomerular filtration followed by tubular reabsorption and lysosomal degradation. In our previous studies with radioiodine-labeled sc(Fv)$_2$, uptake in the kidneys was 21.3 %ID/g 30 min after injection and decreased to 5.4 %ID/g by 4 h (*17,18*). Unlike iodine, which

is rapidly excreted from cells, proteins labeled with active esters containing ^{99m}Tc bind to the ubiquitous intracellular metal-binding proteins and remain trapped in the lysosomes, resulting in a nonspecific accretion of the radionuclide. In the liver, retention was about 2-fold greater for ^{99m}Tc-[sc(Fv)$_2$]$_2$ than for ^{99m}Tc-sc(Fv)$_2$ because the liver is the major organ for catabolism of larger proteins such as IgG and, probably, [sc(Fv)$_2$]$_2$ (*37*). Liver toxicity resulting from high liver uptake does not appear to be a cause for alarm, considering the radioresistance of normal liver cells. Henderson et al. (*38*) showed that in addition to the liver, the spleen is a major site for catabolism of IgGs. The macroautoradiographic images of the mice clearly illustrate the possible use of ^{99m}Tc-labeled multivalent CC49 scFv's as an imaging modality, although liver metastases may be more difficult to detect by ^{99m}Tc-labeled scFv's.

In this study, autoradiography of mice that received ^{99m}Tc-sc(Fv)$_2$ revealed an association between radioactivity and the pancreas. A biodistribution study to investigate this observation found that the %ID per gram of pancreas was $<$0.9 at 6 h after administration. That dimer and its smaller radiolabeled breakdown products are possibly undergoing hepatobiliary excretion and becoming trapped in the head of the pancreas. The biodistribution data for the pancreas support this speculation, as does the observation that all the pancreatic sections were not detected as hot by macroautoradiography (Fig. 5A). ^{99m}Tc-labeled iminodiacetates have been reported to undergo hepatobiliary excretion and to share the pathway of bilirubin and other dye anions, not the bile acids or quaternary amine cations (*39*). This study did not compare the nature of the species with the radiotracer amounts excreted in the bile and urine.

Our approach of indirectly labeling CC49 scFv's with ^{99m}Tc, using SHNH and tricine as the transchelator, can be extended to radiolabeling scFv's with ^{186}Re because these radionuclides have similar chemical properties. This study can be extended to the investigation of the therapeutic potential of ^{186}Re-labeled multivalent scFv's.

CONCLUSION

The divalent and tetravalent scFv's of mAb CC49 were radiolabeled with ^{99m}Tc, and the imaging potential of these novel radioimmunoconjugates was analyzed in a preclinical evaluation. The immunoreactivity and in vitro stability of the ^{99m}Tc-labeled scFv's were studied. Biodistribution studies on athymic mice bearing human colon carcinoma xenografts showed tumor localization with high radiolocalization indices. Macroautoradiography confirmed the imaging potential of these ^{99m}Tc-labeled multivalent scFv's. Because of high tumor-to-blood ratios at early times and rapid clearance, these multivalent scFv's, when radiolabeled with ^{99m}Tc, will have significant diagnostic applications in the field of nuclear medicine.

ACKNOWLEDGMENTS

The authors thank Kay Devish, Jason Jokerst, and Erik Moore for expert technical assistance. The authors acknowledge the Molecular Biology Core Laboratory, University of Nebraska Medical Center, for sequencing studies; the Molecular Interaction Facility, University of Nebraska Medical Center, for BIAcore studies; and Kristi L.W. Berger, communications specialist and editor, Eppley Institute, University of Nebraska Medical Center, for editorial assistance. The monovalent CC49 scFv construct was a generous gift from the National Cancer Institute Laboratory of Tumor Immunology and Biology and the Dow Chemical Co. (Midland, MI). This study was supported by grant DE-FG02-95ER62024 from the U.S. Department of Energy.

REFERENCES

1. Larson SM. Improving the balance between treatment and diagnosis: a role for radioimmunodetection. *Cancer Res.* 1995;55(suppl):5756s–5758s.
2. Britton KE. The development of new radiopharmaceuticals. *Eur J Nucl Med.* 1990;16:373–385.
3. Jain RK. Transport of molecules across tumor vasculature. *Cancer Metastasis Rev.* 1987;6:559–593.
4. Primus FJ, Bennett SJ, Kim EE, DeLand FH, Zahn MC, Goldenberg DM. Circulating immune complexes in cancer patients receiving goat radiolocalizing antibodies to carcinoembryonic antigen. *Cancer Res.* 1980;40:497–501.
5. Behr T, Becker W, Hannappel E, Goldenberg DM, Wolf F. Targeting of liver metastases of colorectal cancer with IgG, F(ab′)$_2$, and Fab′ anti-carcinoembryonic antigen antibodies labeled with ^{99m}Tc: the role of metabolism and kinetics. *Cancer Res.* 1995;55(23 suppl):5777s–5785s.
6. Moffat F Jr, Vargas-Cuba RD, Serafini AN, et al. Radioimmunodetection of colorectal carcinoma using technetium-99m-labeled Fab′ fragments of the IMMU-4 anti-carcinoembryonic antigen monoclonal antibody. *Cancer.* 1994;73:836–845.
7. Becker WS, Behr TM, Cumme F, et al. ^{67}Ga citrate versus ^{99m}Tc-labeled LL2-Fab′ (anti-CD22) fragments in the staging of B-cell non-Hodgkin's lymphoma. *Cancer Res.* 1995;55(23 suppl):5771s–5773s.
8. Fjeld JG, Michaelsen TE, Nustad K. The binding parameters of radiolabelled monoclonal F (ab′)$_2$ and Fab′ fragments relative to immunoglobulin G in reactions with surface-bound antigens. *Eur J Nucl Med.* 1992;19:402–408.
9. Pavlinkova G, Beresford GW, Booth BJ, Batra SK, Colcher D. Pharmacokinetics and biodistribution of engineered single-chain antibody constructs of MAb CC49 in colon carcinoma xenografts. *J Nucl Med.* 1999;40:1536–1546.
10. Bird RE, Hardman KD, Jacobson JW, et al. Single-chain antigen-binding proteins. *Science.* 1988;242:423–426.
11. Colcher D, Bird R, Roselli M, et al. In vivo tumor targeting of a recombinant single-chain antigen-binding protein. *J Natl Cancer Inst.* 1990;82:1191–1197.
12. Milenic DE, Yokota T, Filpula DR, et al. Construction, binding properties, metabolism, and tumor targeting of a single-chain Fv derived from the pancarcinoma monoclonal antibody CC49. *Cancer Res.* 1991;51:6363–6371.
13. Yokota T, Milenic DE, Whitlow M, Schlom J. Rapid tumor penetration of a single-chain Fv and comparison with other immunoglobulin forms. *Cancer Res.* 1992;52:3402–3408.
14. Nieroda CA, Milenic DE, Carrasquillo JA, Scholm J, Greiner JW. Improved tumor radioimmunodetection using a single-chain Fv and gamma-interferon: potential clinical applications for radioimmunoguided surgery and gamma scanning. *Cancer Res.* 1995;55:2858–2865.
15. Courtenay-Luck NS, Epenetos AA, Moore R, et al. Development of primary and secondary immune responses to mouse monoclonal antibodies used in the diagnosis and therapy of malignant neoplasms. *Cancer Res.* 1986;46:6489–6493.
16. Colcher D, Goel A, Pavlinkova G, Beresford G, Booth B, Batra SK. Effects of genetic engineering on the pharmacokinetics of antibodies. *Q J Nucl Med.* 1999;43:132–139.
17. Goel A, Beresford GW, Colcher D, et al. Divalent forms of CC49 single-chain antibody constructs in *Pichia pastoris*: expression, purification, and characterization. *J Biochem.* 2000;127:829–836.
18. Goel A, Colcher D, Baranowska-Kortylewicz J, et al. Genetically engineered tetravalent single-chain Fv of the pancarcinoma monoclonal antibody CC49:

improved biodistribution and potential for therapeutic application. *Cancer Res.* 2000;60:6964–6971.
19. Lowry O, Rosenbrough NJ, Farr AL, Randall RJ. Protein measurement by Folin phenol. *J Biol Chem.* 1951;193:265–275.
20. Laemmli UK. Cleavage of structural proteins during the assembly of the head of bacteriophage T4. *Nature.* 1970;227:680–685.
21. Abrams MJ, Juweid M, tenKate CI, et al. Technetium-99m-human polyclonal IgG radiolabeled via the hydrazino nicotinamide derivative for imaging focal sites of infection in rats. *J Nucl Med.* 1990;31:2022–2028.
22. Huston JS, George AJ, Adams GP, et al. Single-chain Fv radioimmunotargeting. *Q J Nucl Med.* 1996;40:320–333.
23. Mayer A, Chester KA, Flynn AA, Begent RH. Taking engineered anti-CEA antibodies to the clinic. *J Immunol Methods.* 1999;231:261–273.
24. Larson SM, El-Shirbiny AM, Divgi CR, et al. Single chain antigen binding protein (sFv CC49): first human studies in colorectal carcinoma metastatic to liver. *Cancer.* 1997;80:2458–2468.
25. Begent RH, Verhaar MJ, Chester KA, et al. Clinical evidence of efficient tumor targeting based on single-chain Fv antibody selected from a combinatorial library. *Nat Med.* 1996;2:979–984.
26. Verhaar MJ, Keep PA, Hawkins RE, et al. Technetium-99m radiolabeling using a phage-derived single-chain Fv with a C-terminal cysteine. *J Nucl Med.* 1996; 37:868–872.
27. Wu AM, Williams LE, Zieran L, et al. Anti-carcinoembryonic antigen (CEA) diabody for rapid tumor targeting and imaging. *Tumor Targeting.* 1999;4:47–58.
28. Wu AM, Yazaki PJ, Tsai S, et al. High-resolution microPET imaging of carcinoembryonic antigen-positive xenografts by using a copper-64-labeled engineered antibody fragment. *Proc Natl Acad Sci USA.* 2000;97:8495–8500.
29. Claessens RA, Boerman OC, Koenders EB, Oyen WJ, van der Meer JW, Corstens FH. Technetium-99m labelled hydrazinonicotinamido human non-specific polyclonal immunoglobulin G for detection of infectious foci: a comparison with two other technetium-labelled immunoglobulin preparations. *Eur J Nucl Med.* 1996;23:414–421.
30. Steffens MG, Oosterwijk E, Kranenborg MH, et al. In vivo and in vitro characterizations of three ^{99m}Tc-labeled monoclonal antibody G250 preparations. *J Nucl Med.* 1999;40:829–836.
31. Callahan RJ, Barrow SA, Abrams MJ, Rubin RH, Fischman AJ. Biodistribution and dosimetry of technetium-99m-hydrazino nicotinamide IgG: comparison with indium-111-DTPA-IgG. *J Nucl Med.* 1996;37:843–846.
32. Dams ET, Oyen WJ, Boerman OC, et al. Technetium-99m labeled to human immunoglobulin G through the nicotinyl hydrazine derivative: a clinical study. *J Nucl Med.* 1998;39:119–124.
33. Waibel R, Alberto R, Willuda J, et al. Stable one-step technetium-99m labeling of His-tagged recombinant proteins with a novel Tc(I)-carbonyl complex. *Nat Biotechnol.* 1999;17:897–901.
34. Johannsen B, Syhre R, Spies H, Munze R. Chemical and biological characterization of different Tc complexes of cysteine and cysteine derivatives. *J Nucl Med.* 1978;19:816–824.
35. Hnatowich DJ, Mardirossian G, Rusckowski M, Fogarasi M, Virzi F, Winnard P Jr. Directly and indirectly technetium-99m-labeled antibodies: a comparison of in vitro and animal in vivo properties. *J Nucl Med.* 1993;34:109–119.
36. Sanyal S, Banerjee S. Cysteine, a chelating moiety for synthesis of technetium-99m radiopharmaceuticals. II. Attempt to synthesize renal tubular radiopharmaceuticals. *Int J Rad Appl Instrum B.* 1990;17:757–762.
37. Mattes MJ, Griffiths GL, Diril H, Goldenberg DM, Ong GL, Shih LB. Processing of antibody-radioisotope conjugates after binding to the surface of tumor cells. *Cancer.* 1994;73:787–793.
38. Henderson LA, Baynes JW, Thorpe SR. Identification of the sites of IgG catabolism in the rat. *Arch Biochem Biophys.* 1982;215:1–11.
39. Harvey E, Loberg M, Ryan J, Sikorski S, Faith W, Cooper M. Hepatic clearance mechanism of Tc-99m-HIDA and its effect on quantitation of hepatobiliary function: concise communication. *J Nucl Med.* 1979;20:310–313.
40. Goel A, Colcher D, Koo J, Booth BJM, Pavlinkova G, Batra SK. Relative position of the hexahistidine tag effects binding properties of a tumor-associated single-chain Fv construct. *Biochim Biophys Acta.* 2000;1523:13–20.

JNM The Journal of NUCLEAR MEDICINE

^{99m}Tc-Labeled Divalent and Tetravalent CC49 Single-Chain Fv's: Novel Imaging Agents for Rapid In Vivo Localization of Human Colon Carcinoma

Apollina Goel, Janina Baranowska-Kortylewicz, Steven H. Hinrichs, James Wisecarver, Gabriela Pavlinkova, Sam Augustine, David Colcher, Barbara J.M. Booth and Surinder K. Batra

J Nucl Med. 2001;42:1519-1527.

The Journal of Nuclear Medicine is published monthly.
SNMMI | Society of Nuclear Medicine and Molecular Imaging
1850 Samuel Morse Drive, Reston, VA 20190.
(Print ISSN: 0161-5505, Online ISSN: 2159-662X)

SNMMI SOCIETY OF NUCLEAR MEDICINE AND MOLECULAR IMAGING